Nanomed Res J 11(2):167-176, Spring 2026

RESEARCH ARTICLE

Synthesis of Silibinin-Loaded Cellulose Nanocrystals Modified with Cetyltrimethylammonium Bromide (CTAB) and Investigation of its Cytotoxic Effects on MCF-7 Breast Cancer Cells

Nahid Irani, Yashar Gholitabar Omrani, Masoud Homayuni-Tabrizi, Ali Es-haghi*

Department of Biology, Ma.C., Islamic Azad University, Mashhad, Iran

ARTICLE INFO

Article History:
Received: 2026-01-26
Revised: 2026-04-28
Accepted: 2026-05-09

Keywords:
Cellulose nanocrystals
CTAB
Breast cancer
Silibinin

ABSTRACT

Anticancer drug delivery remains a challenge of paramount importance in oncology. Recently, cellulose nanocrystals (CNC) have been used to optimize drug dispersion and loading efficiency. The goal of this research is to modify CNC with cetyltrimethylammonium bromide (CTAB) and loading silibinin into it, to deliver the silibinin to breast cancer cells. Nanoparticles were synthesized and its surface modify by CTAB then, silibinin was loaded into it. SIL-CNC-CTAB were analyzed using special techniques for nanoparticle analysis such as dynamic light scattering (DLS), transmission electron microscopy (TEM), fourier transform infrared spectroscopy (FTIR) and zeta potential measurement. Anticancer effects were evaluated through the MTT assay. Apoptosis detection was evaluated by acridine orange/propidium iodide (AO/PI) staining. The obtain results showed a hydrodynamic diameter of NP was 335.65 nm with a poly dispersity index (PDI) of 0.35. Zeta potential of was -26.66±6.32 mV. Encapsulation efficiency determined 83.8% of silibinin loaded on CNC-CTAB. Breast cancer MCF-7 cells exposed to silibinin-loaded CTAB-modified CNCs revealed significant toxicity with an IC50 value of 107 µg/mL and promotion of apoptotic changes confirmed by AO/PI analysis. According to the data of the present study, silibinin-loaded CTAB-modified CNCs could prevent the progress and proliferation of MCF-7 breast cancer cells.

How to cite this article
Irani N, Gholitabar Omrani Y, Homayuni-Tabrizi M, Es-haghi A. Synthesis of Silibinin-Loaded Cellulose Nanocrystals Modified with Cetyltrimethylammonium Bromide (CTAB) And Investigation of its Cytotoxic Effects on MCF-7 Breast Cancer Cells. Nanomed Res J, 2026; 11(2): 167-176. DOI: 10.22034/nmrj.2026.02.007

INTRODUCTION

Despite medical and technological advances, cancer and infections continues to claim tens of millions of lives each year [1-4]. Scientists have been investigating the disease long time, and even with enhanced treatment items, existing remedial such as chemotherapy drugs, provoke severe side effects [5-9]. Patients suffering from advanced cancers suffer greatly from therapy-related ailments, particularly when their disease relapses, so they are forced to undergo more aggressive treatments [10-13]. The use of chemotherapy without specific targeting mechanisms leads to the elimination of both cancer and non-cancer cells, thus causing systemic toxicity. Breast cancer (BC) is one of the most common kinds of cancer responsible for remarkable mortality among both men and women each year. Despite notable developments in initial detection and appropriate treatment, BC remains the chief cause of cancer-related death and disability among women [14-18]. This figure is further aggravated due to the toxic effects of chemotherapeutics used to treat BC.

Currently, a restrictive factor in chemotherapy is the deficiency of selectivity of drugs against cancer cells [19]. In addition, most anticancer drugs have a low therapeutic index, exaggerating their toxic side effects. For the duration of chemotherapy, some cancer cells develop resistance to treatment, requiring dose escalation or combinational therapy for better clinical outcomes at the cost of more side effects [20-

* Corresponding Author Email: *Ali.Eshaghi@iau.ac.ir*

22]. In order to resolve these problems, a range of drug delivery structures have been established [23-25]. In recent years, cellulose nanocrystals (CNCs) have been considered as promising nanomaterials for drug delivery applications [26, 27]. CNCs derived from renewable resources offer several advantages, including high surface area, biocompatibility, and the capability to be improved for specific purposes [28, 29]. Introducing positive charges on the surface of CNCs through CTAB modification enhances their interaction with therapeutic agents and biological systems [30-32]. This approach helps improve drug loading and controlled release, offering greater drug loading and delivery efficiency and improving the physical and chemical properties of CNCs. Effective anticancer drug delivery residues a main challenge in oncology, and novel drug carriers, such as CTAB-modified CNCs, have offered promising potential to address these challenges.

Silibinin is a polyphenol which antioxidant and antitumor activities have been established. Recently, several works have been done to assess the anticancer effects of polyphenols and silibinin, confirming its ability to inhibit cancer cells' growth by inducing apoptosis via yet to be fully disclosed molecular mechanisms [8, 33-35]. Silibinin has shown therapeutic potential against a variety of cancer cells via intensifying free radical-induced cellular damage, suppressing cell cycle progression, and promoting anti-angiogenic properties [36-38]. A considerable trouble in the transfer of this drug to the cancer cells is, the extremely poor aqueous solubility. So far, no research has been conducted on silibinin-loaded CNC-CTAB on breast cancer. Therefore, in this study, we synthetized and characterized silibinin-loaded cellulose nanocrystals modified with CTAB (SIL- CNC-CTAB) and evaluated its anti-cancer effects on the breast cancer cell line.

MATERIALS AND METHODS

Materials

MCF-7 breast cancer cell line was acquired from Pasteur Institute of Iran. Trypsin-EDTA, RPMI164 culture medium, antibiotic, and FBS were purchased from GIBCO. MTT reagent, CTAB, propidium iodide (PI), and acridine orange (AO) and silibinin were provided from sigma-aldrich. DMSO solvent was purchased from Thermo Fisher Scientific (USA).

Methods

Synthesis of SIL- CNC-CTAB NPs

To improve CNC with CTAB ,100 mg of dried CNC was sonicated in 20 mL of deionized water for 15 minutes. Also 100 mg of CTAB was dissolved in 10 mL of deionized water Separately, and added to the CNC suspension. The mixture was stirred at 50°C for 2 hours to allow CTAB adsorption. Afterward, the CTAB-modified CNC NPs were collected using centrifugation (10,000× g) for 10 min, washed 3-times with deionized water. For Loading of silibinin to CNC-CTAB, silibinin (10 mg) was solvated in DMSO and added drop by drop to a CNC/CTAB suspension whit stirring for 2 hours, allowing the adsorption of silibinin onto the NPs. Then, by centrifugation silibinin -loaded NPs were precipitated and washed with deionized water several time to remove free silibinin molecules. Finally, silibinin /CNC/CTAB/ NPs gathering, washing by deionized water and put in freeze-dried for next used.

Characterization of CNCs

The average size (nm) and particle dispersion index (PDI) were done by DLS and surface charge were determined using Zetasizer instrument (Nano-ZS, Malvern, UK). Samples were dispersed in deionized water and sonicated for 5-min to ensure uniform suspension. Measurements were taken at 25°C with a backscattering angle of 173. Z-potential amounts were conducted to assess electrophoretic mobility and surface charge. A FESEM (JEOL, Japan) was used to examine the appearance of the nanoparticles. For taken a picture, a drop of the NPs suspension put down on the carbon coated copper gird and drying in the air. FTIR study was utilized to recognize functional groups on the surface of nanoparticle (Perkin Elmer, Walthman, MA, USA). For this purpose, SIL-CNC-CTAB was mixed with potassium bromide (KBr) and then compacted into tablets whose spectra were measured at 4000-400 cm^{-1} employing an FT-IR spectrophotometer.

Determination of the Encapsulation Efficiency

The encapsulation efficiency of silibinin in SIL-CNC-CTAB NPs was measured by utilizing a Shimadzu UV-1800 UV-Vis spectrophotometer at 280 nm (UV Spectrophotometer UV-1800, Shimadzu, Japan). For this purpose, first, standard calibration curve of silibinin in methanol was drown. Then, 300 µL of NP suspension was lyophilized to make the samples, and the dry powder

was reconstituted in 2 mL of methanol. The mixture underwent bath sonication at 37°C for 15 min, next centrifugation (12,000 g) for 15 minutes at 4°C to eliminate particulate matter. The supernatant was filtered for analysis. Encapsulation efficacy (%) was evaluated by: (amount of silibinin loaded in NPs / amount of silibinin initially added) × 100.

Silibinin Release Assay

The drug release profile of silibinin from SIL-CNC-CTAB was tested by immersing a specific quantity of the formulation in 10 ml of PBS. Samples were taken at predetermined intervals (1, 3, 6, 12, 24, 48 and 72 h) and centrifuged to detached the released silibinin from the SIL-CNC-CTAB. The supernatant was then examined at 289 nm to calculate the amount of silibinin released.

Cytotoxicity Assay

To investigate the cytotoxicity of Sil-CNC-CTAB, the MCF-7 breast cancer cell line was used. First, the cells were thawed after being recovered from a nitrogen tank and placed in the laboratory environment to reach ambient temperature. Then an appropriate cell culture medium was added to cells, and the suspension was transferred to a flask to be incubated under 5% CO2 and 37°C. The MTT test is one of the most popular methods used to check cellular viability. MCF-7 cells were cultured in a 96-well plate where they were exposed to SIL-CNC-CTAB for a specific time period. Then 40 µl of the MTT solution (4 mg/ml) was added to each well. Then the plates were wrapped inside a foil, returned to the incubator, and kept for four hours at 37°C. At this stage, living cells transform the solution into a purple crystal, while the solution remains yellow or colorless in non-alive (i.e., no metabolic activity) cells. In the next step, the medium was drained, and the formazan product was dissolved by adding 100 µl of DMSO. Finally, color intensity was determined by a plate reader at a wavelength of 570 nm. Using a standard curve, the 48-hour IC50 of silibinin was determined. Cell viability at each concentration was calculated according to a previous study. The IC50 value was designated as the concentration at which 50% of cells were alive, and viability percentage was used to assess dose-dependent toxicity.

Cell staining by acridine orange/propidium iodide (AO/PI)

AO/PI dual labeling was used to investigate the ability of SIL-CNC-CTAB to trigger apoptosis in MCF-7 cells. A 24-well plate was cultured with 4×10^5 cells per well, and the cells were incubated for 24 hours. The cells were then treated with different doses of SIL-CNC-CTAB adjusted according to the IC50 value of 107 µg/mL. After that, the cells were stained with 100 µg/ml of AO/PI in a 1:1 ratio for five minutes. Finally, apoptosis was detected by inspecting cells under a fluorescent microscope.

Statistical Data Analysis

All tests were conducted 3-times, and data were expressed as mean ± standard error of the mean. One-way ANOVA and the LSD post-hoc test were used for inferential evaluations using SPSS software (version 21.0) at a significance level of less than 0.05. Error bars on graphs represented standard deviations; a 5% confidence level was considered for calculations.

RESULTS

In this study, DLS-derived average particle size, particle dispersion index (PDI), zeta potential, and SEM analysis were used to physicochemically characterize the synthesized nanocrystals. According to Figure 1A, a unique monodisperse peak at around 335 nm indicated consistent particle size distribution with little agglomeration.

Figure 1B depicts the zeta potential of the synthesized SIL-CNC-CTAB NPs. Z-potential is a technique for measuring of the surface electrical charge of particles in a liquid suspension and can provide important information about the stability of colloidal systems or nanoparticles. In our study, the zeta potential of the nanocrystals was -26.66±6.32 mV. The zeta potential suggested that the synthesized nanoparticles had appropriate stability. A micrograph of the nanocrystals taken by scanning electron microscopy (SEM) showed the high-resolution fibrous morphology of the formulation (Fig 1C).

FTIR spectra

Numerous unique peaks were visible in the FTIR spectrum of CNC-CTAB nanoparticles (Fig. 2). FTIR spectra of pure nanocrystalline cellulose (NCC), CTAB-modified NCC and silibinine-loaded NCC-CTAB samples clearly show the successful structural and chemical changes during the modification and pharmaceutical process. In the pure NCC complex, the broad and strong band in the range of 3200–3500 cm^{-1} is assigned to the

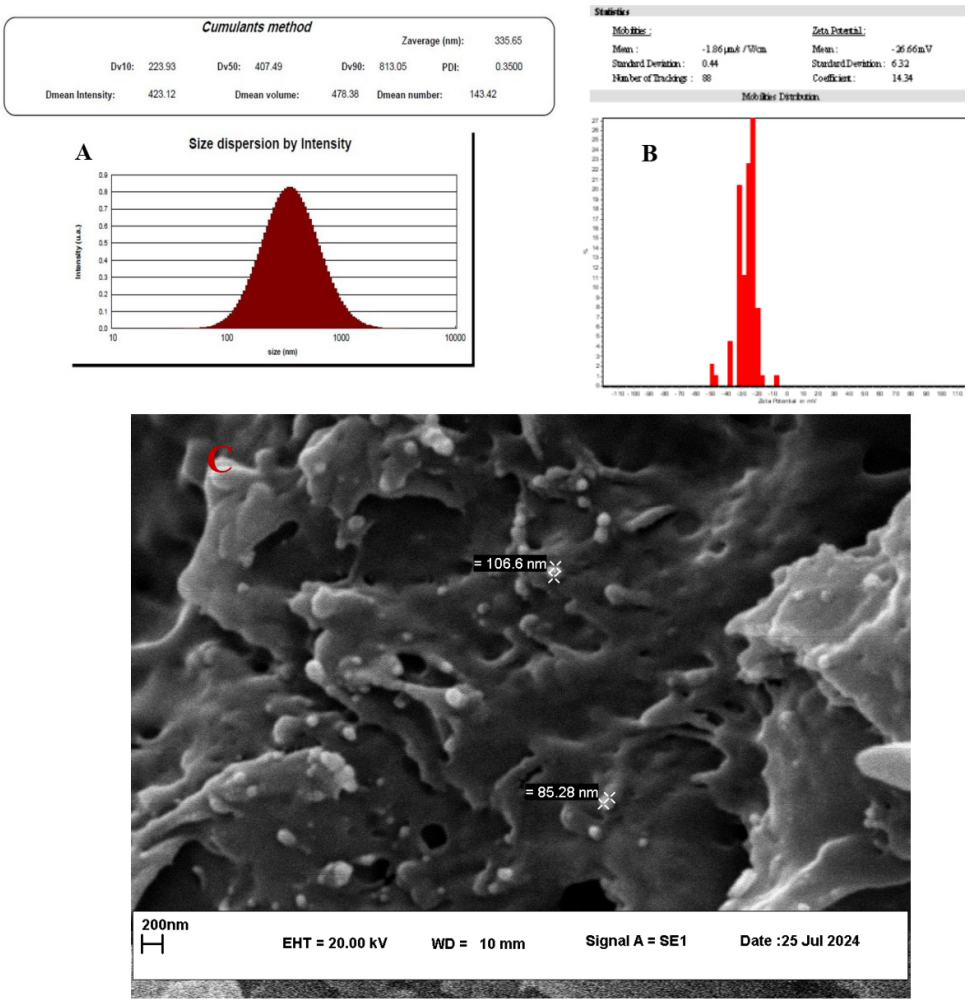

Fig. 1. The physicochemical features of the synthesized nanocrysals. (A) Average particle size and other characteristics, (B) Zeta potential, and (C) SEM micrograph.

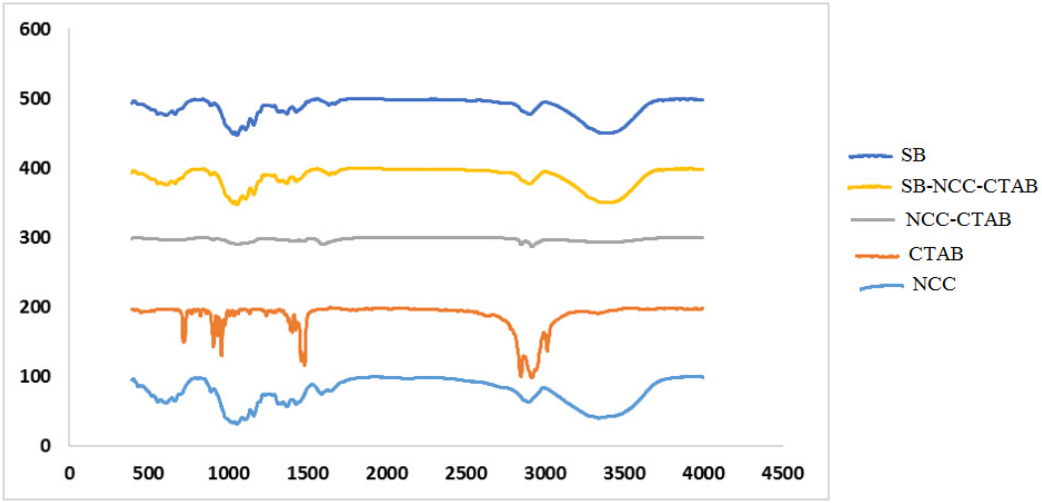

Fig. 2. FTIR spectra of pure nanocrystalline cellulose (NCC), Silibinin (SB), CTAB, CTAB-modified NCC and silibinine-loaded NCC-CTAB samples.

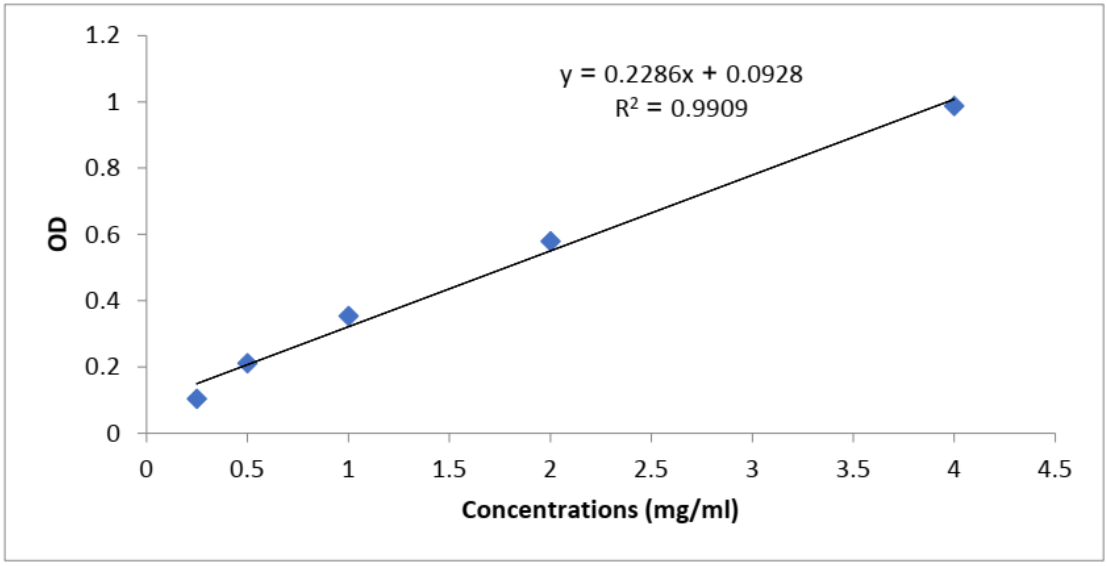

Fig. 3. Standard calibration curve of silibinin.

stretching of hydroxyl groups (O–H), indicating the strong hydrogen bonds and high hydrophilic nature of the cellulose nanocrystals. The peak around 2900 and 100 cm^{-1} is related to the C–H stretching in the aliphatic chains of the cells. The strong band in the region of 1100–110 cm^{-1} is attributed to the C–O–C (ether bond) and C–O stretching in the pyranose ring of the cells, which becomes the fingerprint characteristic of the cellulose structure. Also, the peak around 1640 cm^{-1} is attributed to the O–H bending of adsorbed water in the lower regions (500–900 cm^{-1}).

After the NCC surface modification with the ionic surfactant CTAB, the original cell structure is preserved but some obvious changes are observed. The new or enhanced peaks in the range of 2850–2920 cm^{-1} are assigned to the symmetric and asymmetric C–H stretching of the long alkyl chain in CTAB, which is the most important indication of the success of the hydrophobic modification of the NCC surface. Hydrogen reduction is responsible for O–H band at 3200–3500 cm^{-1} due to the hydrophobic coating of CTAB. The peak around 1470–1480 cm^{-1} is also attributed to the C–N vibration or N^{+}-CH3 bending of the quaternary ammonium group of CTAB. These CTAB modifications cause CTAB to be adsorbed onto the surface through electrostatic (with the negative sulfate groups of NCC) and hydrophobic interactions, imparting ionic and hydrophobic properties to the nanoparticles.

In the spectrum of silibinin-loaded NCC-CTAB, the main features of NCC-CTAB are still preserved, indicating no major disruption of the basic structure. The O–H band at 3200–3500 cm^{-1} broadens, which is caused by the addition of phenolic hydroxyl groups of silibinin. The further enhancement of the C–H peaks at 2850–2950 cm^{-1} is due to the alkyl groups of CTAB and the aliphatic moieties of silibinin. The peak at around 1660 cm^{-1} is assigned to the C=O (carbonyl group) stretching in the flavonolignan structure of silibinin, which is the key indication of the successful synthesis. Also, aromatic C=C vibrations are observed in the range of 1430–1510 cm^{-1} from the benzopyranone rings of silibinin. The absence of strong new peaks in the fingerprint region (500–1500 cm^{-1}) suggests structural loading (adsorption or encapsulation) of silibinin in the hydrophobic domains created by CTAB rather than covalent bond formation. The C–H reference in the lower and strong C–H regions is consistent with the features of CTAB (C–H peaks at 2850–2920 cm^{-1} and C–N at ~1470 cm^{-1}) or silibinin (phenolic O–H at ~3370 cm^{-1}, C=660 cm^{-1}, and C=60~O) cm^{-1}).

Encapsulation Efficacy

The quantification of silibinin was done by a calibration curve described by the linear equation y = 0.2286x + 0.0928, with an excellent correlation coefficient (R^2 = 0.9909), demonstrating the reliability and precision of the analytical method (Fig. 3) The encapsulation efficiency of silibinin

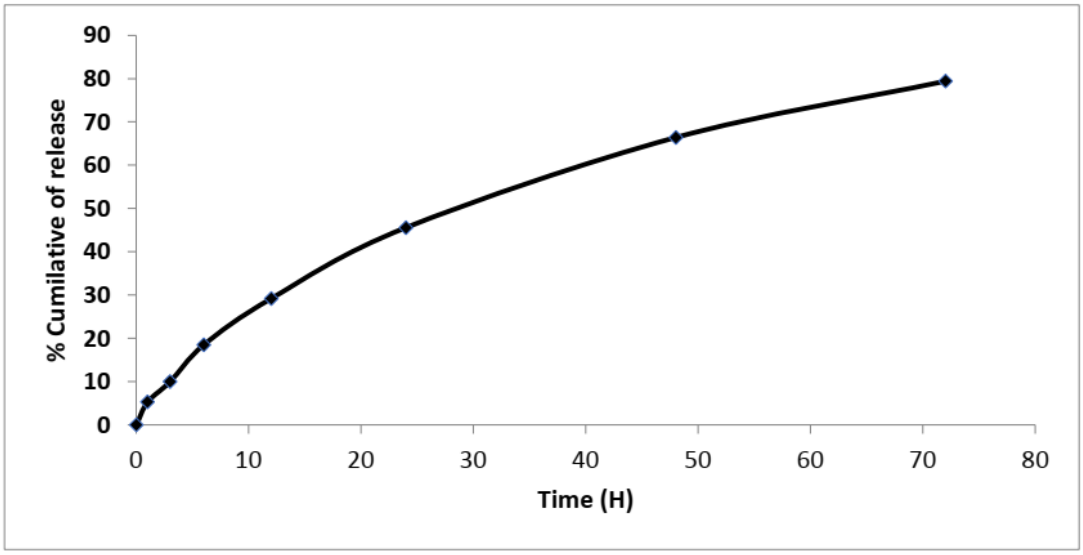

Fig. 4. Silibinin release form SIL-CNC-CTAB NPs.

into the SIL-CNC-CTAB NPs was determined to be 83.81%, indicating a high loading capacity of the nanocarrier system. These results confirm the effective incorporation of silibinin within the nanoparticulate matrix.

Silibinin release form SIL-CNC-CTAB NPs

The cumulative release of SIL from SIL-CNC-CTAB NPs progressed with time, reaching 0, 5.3, 10, 18.5, 29.2, 45.6, 66.4, and 79.4% at 0, 1, 3, 6, 12, 24, 48, and 72 hours, respectively (Fig 4).

Cytotoxicity Study

In order to assess the therapeutic efficacy of SIL-CNC-CTAB, the cytotoxic properties of various concentrations of the nanocrystals were measured by the MTT test. Due to its simplicity and accuracy, this assay is widely employed to investigate the cytotoxic effects of drugs on living cells in pharmacology research [39-41]. Here, MCF-7 cells were treated with SIL-CNC-CTAB for 48 h, revealing substantial dose-dependent cytotoxicity at the dose of 7.8, 15.6, 31.2, 62.5, 125, 250, and 500 µg/mL (Fig 5), where IC50 was determined as 107 µg/mL.

AO/PI Staining

Apoptosis was measured by AO/PI staining, which is a common technique utilized in cell biology and microbiology to detect apoptotic changes in cells via fluorescence microscopy or flow cytometry [40, 42]. Based on our results, MCF-7 cells treated with SIL-CNC-CTAB at the concentrations of 7, 107, and 307 µg/mL exhibited changes characteristic of apoptotic cells (for example, morphological changes such as shrinkage, transformation into a spherical shape, plasma membrane budding). Control cells showed uniform green fluorescence from the nucleus and cytoplasm, exhibiting predominant green fluorescence (AO^+/PI^-), indicating intact membrane integrity and viable cells. At 7 µg/mL (Fig. 6), early apoptotic cells (AO^+/PI^+) displaying both green and orange-red fluorescence became apparent, while late apoptotic cells (AO^-/PI^+) with intense red nuclear staining dominated at higher concentrations of 107 µg/mL (Fig.) and 307 µg/mL (Fig.6). In cancer cells treated with SIL-CNC-CTAB displayed red fluorescence, indicating the penetration of PI dye into damaged apoptotic cells. Fluorescence images confirmed changes in nucleus density and fragmentation in cells treated with nanocrystals. In a concentration-dependent manner, bright spots appeared at the nuclei of apoptotic cells, reflecting dose-dependent apoptosis. These findings collectively demonstrate the dose-dependent cytotoxic efficacy of the NPs through induction of programmed cell death.

DISCUSSION

This work examined the properties of SIL-CNC-CTAB NPs on MCF-7 breast cancer cells Ray et al. (2024) showed that silibinin exhibited antitumor

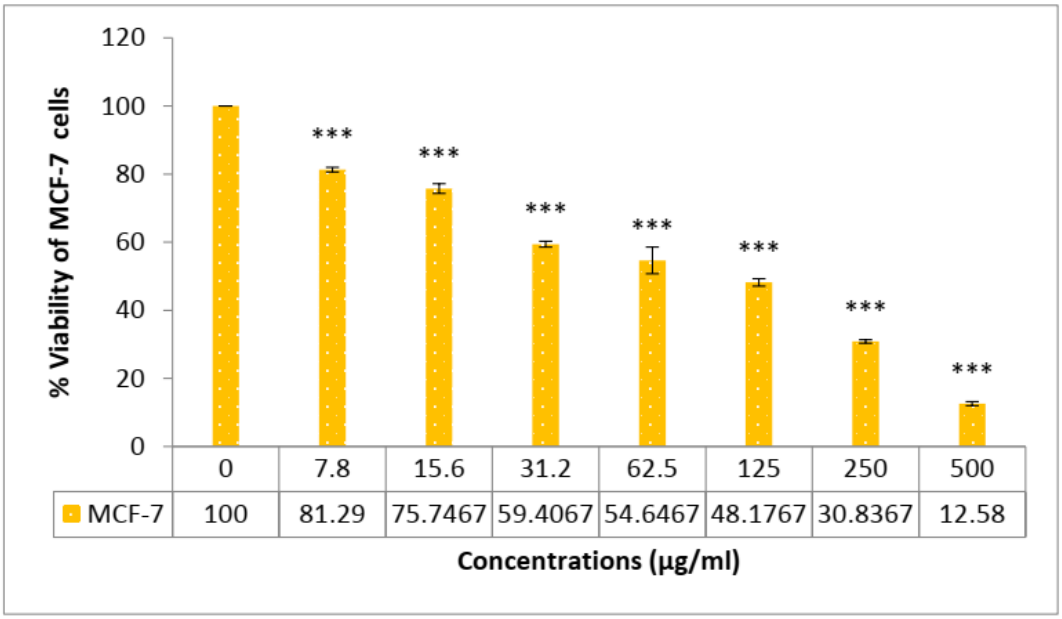

Fig. 5. The cytotoxicity of different concentrations of synthetic nanocrystals against the MCF-7 cell line. SIL-CNC-CTAB NP reduced cancerous cell viability in a dose-dependently way, showing the maximum cytotoxicity. Data are presented as mean ± SEM. The test was done in triplicate and *** indicated that the $p<0.001$ compared to the control (0).

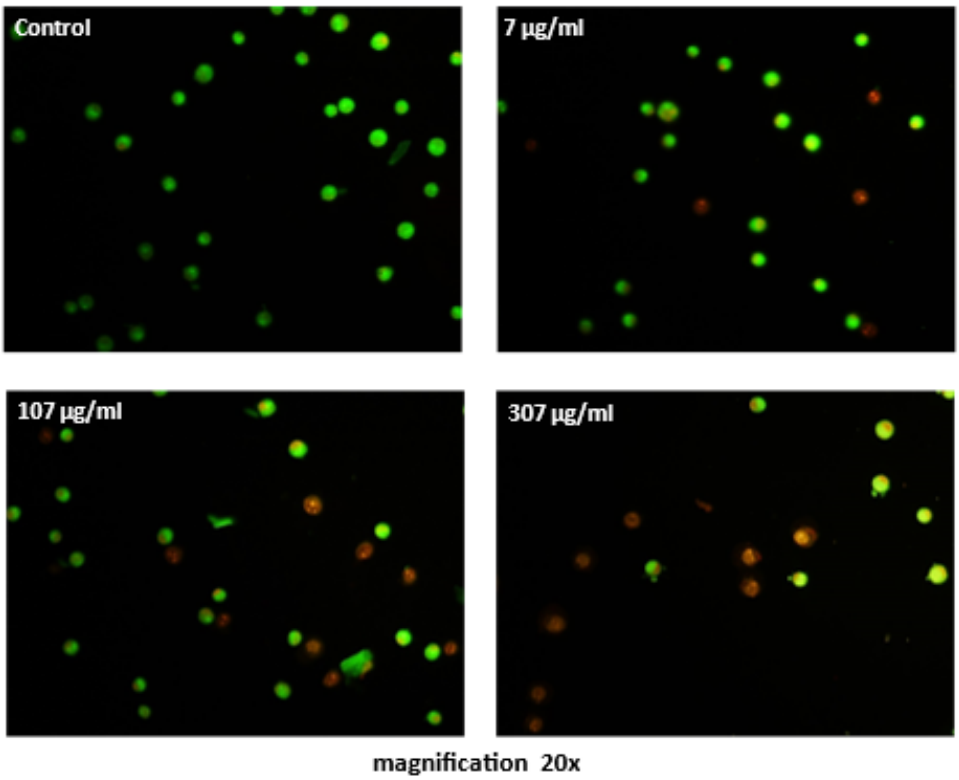

Fig. 6. AO/PI staining analysis displays dose-dependent apoptosis induction in MCF-7 cells treated with SIL-CNC-CTAB NPs. (A) Untreated controls display green fluorescence (viable cells). (B) At 7 µg/mL, early apoptotic cells show mixed green and orange-red fluorescence (membrane alterations). (C) At 107 µg/mL, late apoptotic cells are evident with intense red staining (membrane permeabilization and nuclear condensation). (D) Late apoptotic cells dominate at 307 µg/mL with strong red fluorescence, indicating extensive nuclear fragmentation and membrane disruption.

properties against several kinds of cancer cells. Silibinin containing special properties including, antioxidant, anti-proliferative, and anti-metastatic properties, which make it a good candidate for treatment of cancer cells. One of the crucial procedures for anticancer activity of silibinin is its capability to regulate several signaling paths which require for cancer progress. It has been shown the activation of numerous oncogenic ways, such as PI3K/Akt, NF-κB, and MAPK pathways inhibited by silibinin, thus cancer cell proliferation and cell cycle promotion inhibit, along with promoting apoptosis. Therefore, silibinin has a considerable possibilities for effective therapeutic for cancer treatment [43]. The cytotoxicity and apoptotic effects observed against cancer cells treated with silibinin were consistent with the data of the present study. Kumari et al. (2023) fabricated CNC from lignocellulosic waste of lemongrass by enzymatic hydrolysis and showed that curcumin encapsulated CNCs, while being stable for up to 24 hours and in all physiological pH conditions compared to pure curcumin, could support gradual *in vitro* release of curcumin at different pH conditions mimicking tumor microenvironment. The MTT assay established the non-cytotoxic or hemolytic effects of CNCs on A431 cells and human erythrocytes at various dose (2–10 μg/mL). Finally, CNCs loaded with curcumin exhibited higher *in vitro* cell toxicity and enhanced cellular uptake compared to free curcumin [44]. The above findings were in line with the consequences of this work, indicating increased cytotoxicity of cellulose nanocrystals against cancerous cells. In a study by Xing et al. (2023), CNC and polydopamine (PDA) coated DMON were prepared to develop bio-compatible pH-responsive nanocarriers for the effective delivery of paclitaxel. The modified CNC was expected to inhibit drug-leakage while confirming effective drug release from the nanocarrier at the tumor place. PDA was incorporated as an external coating, a biocompatible molecule that could enhance cellular uptake by supporting cell adhesion and enabling drug-stimulated response release. This nanocarrier exhibited excellent cellular uptake and pH-responsive release activities, with the cumulative drug release at pH 5.5 reaching 80.59% within 85 hours [45]. In our study, based on the results of AO/PI analysis, the cells treated with SIL-CNC-CTAB at the dose of 7, 107, and 307 μg/mL exhibited apoptotic features. In chemodynamic cancer therapy, CNC-coated drug delivery systems seem to provide an effective and controlled release of drugs. Sajjadiyan et al. (2016) constructed nanoparticles containing silibinin and investigated their effects on the MCF-10A human breast cancer cell line in order to improve the drug's poor bioavailability at the tumor site [46]. In the recent study, SIL encapsulated in nanoniosomal particles modified with polyethylene glycol showed higher cytotoxic effects than free silibinin on the MCF 10A cell line, suggesting this platform as an effective drug delivery system for breast cancer treatments. These findings were consistent with our observation in the present study. Pirouzpanah et al., in a 2015 study, investigated the apoptotic and growth inhibitory effects of silibinin (25 to 800 μmol for 24, 48, and 72 hours) on the MCF-7 cell line and reported that at a dose of 200 μmol for 24 hours (48-hour IC_{50}: 148 μmol), the drug had significant dose- and time-dependent effects on cell growth and apoptosis, accompanied by P53 overexpression [47]. Accordingly, this increase in toxicity against MCF-7 cancer cells treated with silibinin was consistent with the outcomes of this work. Likewise, Mahmoodi et al. declared that silibinin, as a polyphenol with antioxidant and anticancer properties, meaningfully decreased the viability of T47D breast cancer cells [48]. Another study conducted by Jackson et al. in 2011 revealed that CTAB-modified CNCs were proficient in binding and controlled release of anticancer drugs. In the recent report, CNCs prepared by acid hydrolysis had nanoscopic dimensions, showed a high degree of crystallinity, and could bind significant amounts of water-soluble and ionizable drugs (i.e., doxorubicin and tetracycline), which were quickly released during the one day. CTAB bound to CNC surface increased the zeta potential from 0 to -55 mV in a concentration-dependent manner, boosting their capacity for carrying and gradually releasing hydrophobic anticancer drugs. CNC-CTAB complexes were able to effectively penetrate into the KU-7 cell line [49]. The above findings were consistent with the consequences of the current work, advocating for the potential applicability of CNCs as drug carriers.

CONCLUSION

According to the data obtain from the present study, CNCs modified with CTAB were capable to prevent the cell growing and proliferation of MCF-7. This phenomenon was associated with concentration-dependent cytotoxicity and

pro-apoptotic effects. These nanoparticles, like polymeric nanoparticles, showed a slow-release profile, allowing for possible drug accumulation in the tumor site. While CTAB-modified CNCs caused significant toxicity against cancer cells, they were compatible with normal cells in vitro. Based on our observations, CNCs have great potential in the field of cancer treatment caused by their distinctive properties such as capacity for surface modifications, allowing the loading and controlled release of chemotherapeutics.

CONFLICTS OF INTEREST

The authors have no conflicts of interest to declare.

REFERENCES

1. Bagherian MS, et al. Antimicrobial and antibiofilm properties of selenium-chitosan-loaded salicylic acid nanoparticles for the removal of emerging contaminants from bacterial pathogens. World J Microbiol Biotechnol. 2024;40(3):86. https://doi.org/10.1007/s11274-024-03917-z
2. Khiabani Y, et al. In-silico analysis of CYP1A2 (cytochrome P450 1A2) missense mutations: Implications for pharmacogenetics. Heliyon. 2025;11(6):e43312. https://doi.org/10.1016/j.heliyon.2025.e42955
3. Hussain QM, et al. Biosynthesis and characterization of selenium nanoparticles using Ceratonia Siliqua and evaluation of its antimicrobial properties. Nanomed Res J. 2024;9(2):195-205.
4. Es-Haghi A, Amiri MS, Taghavizadeh Yazdi ME. Ferula latisecta gels for synthesis of zinc/silver binary nanoparticles: antibacterial effects against gram-negative and gram-positive bacteria and physicochemical characteristics. BMC Biotechnol. 2024;24(1):51. https://doi.org/10.1186/s12896-024-00878-x
5. Es-haghi A, et al. The Expression of Antioxidant Genes and Cytotoxicity of Biosynthesized Cerium Oxide Nanoparticles Against Hepatic Carcinoma Cell Line. Avicenna J Med Biochem. 2019;7(1):16-20. https://doi.org/10.34172/ajmb.2019.04
6. Taghavizadeh Yazdi ME, Amiri MS, Darroudi M. Biopolymers in the Synthesis of Different Nanostructures. In: Nanostructures. 2020.
7. Yazdi MET, et al. Ultrasound-based synthesis of ZnO·Ag2O3 nanocomposite: characterization and evaluation of its antimicrobial and anticancer properties. Res Chem Intermed. 2021;47(3):1285-1296. https://doi.org/10.1007/s11164-020-04355-w
8. Hashemzadeh A, et al. Polyphenol-Functionalized Metal-Organic Frameworks: A Strategic Platform for Advanced Cancer Drug Delivery and Synergistic Therapy. Mater Res Bull. 2025;180:113778. https://doi.org/10.1016/j.materresbull.2025.113778
9. Ebadi A, et al. Synthesis and Application of Chitosan-Salicylic Acid Magnetic Nanoparticles in Colon Cancer Cells. Nano Select. 2025;6(8):e70086. https://doi.org/10.1002/nano.70086
10. Lustberg MB, et al. Mitigating long-term and delayed adverse events associated with cancer treatment: implications for survivorship. Nat Rev Clin Oncol. 2023;20(8):527-542. https://doi.org/10.1038/s41571-023-00776-9
11. Mohammadzadeh V, et al. Poly-γ-glutamic acid nanoparticles as adjuvant and antigen carrier system for cancer vaccination. J Control Release. 2023;362:278-296. https://doi.org/10.1016/j.jconrel.2023.08.049
12. Taghavizadeh Yazdi ME, et al. Recent Advances in Nanoparticles Applications in Respiratory Disorders, a Review. Front Pharmacol. 2023;14:1059343. https://doi.org/10.3389/fphar.2023.1059343
13. Bakhtiari FSE, Ghorbani Y, Amiri N, Movahedi Roudi S, Gohari Moghaddam F, Zare-Zardini H, et al. Egg white albumin and gelatin scaffolds incorporating silver-copper nanoparticles for enhancing anticancer activity against hepatocellular carcinoma. Results Chem. 2026;23:101985. https://doi.org/10.1016/j.rechem.2026.103140
14. Farhangi MJ, et al. MOF-Mediated Synthesis of CuO/CeO2 Composite Nanoparticles: Characterization and Estimation of the Cellular Toxicity against Breast Cancer Cell Line (MCF-7). J Funct Biomater. 2021;12(4):53. https://doi.org/10.3390/jfb12040053
15. Shakerimanesh K, et al. Biomimetic synthesis and characterisation of homogeneous gold nanoparticles and estimation of its cytotoxicity against breast cancer cell line. Mater Technol. 2022;37(10):1-8. https://doi.org/10.1080/10667857.2022.2081287
16. Mousavi-Kouhi SM, et al. Plant Gel-Mediated Synthesis of Gold-Coated Nanoceria Using Ferula gummosa: Characterization and Estimation of Its Cellular Toxicity toward Breast Cancer Cell Lines. J Funct Biomater. 2023;14(7):332. https://doi.org/10.3390/jfb14070332
17. Rahimi E, et al. Chitosan coated copper/silver oxide nanoparticles as carriers of breast anticancer drug: Cyclin D1/P53 expressions and cytotoxicity studies. Inorg Chem Commun. 2024;159:111581. https://doi.org/10.1016/j.inoche.2023.111581
18. Ramezani Moghadam K, et al. Eco-friendly synthesis of gold nanoparticles using Gracilaria gracilis with antioxidant potential and biocompatibility. Sci Rep. 2026;16:15678. https://doi.org/10.1038/s41598-026-38677-3
19. Mousavi-Kouhi SM, et al. Silver-zinc oxide nanocomposite: From synthesis to antimicrobial and anticancer properties. Ceram Int. 2021;47(15):21490-21497. https://doi.org/10.1016/j.ceramint.2021.04.160
20. Leary M, et al. Sensitization of drug resistant cancer cells: a matter of combination therapy. Cancers (Basel). 2018;10(12):483. https://doi.org/10.3390/cancers10120483
21. Rebucci M, Michiels C. Molecular aspects of cancer cell resistance to chemotherapy. Biochem Pharmacol. 2013;85(9):1219-1226. https://doi.org/10.1016/j.bcp.2013.02.017
22. Ortiz M, et al. Mechanisms of chemotherapy resistance in ovarian cancer. Cancer Drug Resist. 2022;5(2):304-321. https://doi.org/10.20517/cdr.2021.147
23. Ghorani-Azam A, et al. Resveratrol-Mediated Gold-Nanoceria Synthesis as Green Nanomedicine for Phytotherapy of Hepatocellular Carcinoma. Front Biosci (Landmark Ed). 2022;27(8):227. https://doi.org/10.31083/j.fbl2708227

24. Eslamieh-Ei FM, et al. Synthesis and its characterisation of selenium/silver/chitosan and cellular toxicity against liver carcinoma cells studies. Nat Prod Res. 2023;38(12):1-9. https://doi.org/10.1080/14786419.2023.2256023
25. Zarharan H, et al. The anti-angiogenesis and antioxidant activity of chitosan-mediated synthesized selenium-gold nanostructure. Arab J Chem. 2023;16(7):104806. https://doi.org/10.1016/j.arabjc.2023.104806
26. Wan W, et al. Polyethyleneimine coated cellulose nanocrystals decorated with 3-carboxyphenylboronic acid as a pH-responsive nanocarrier for targeted drug delivery. Cellulose. 2025;32(6):1-15. https://doi.org/10.1007/s10570-025-06684-8
27. Ahmed S, Khan RA, Rashid TU. Cellulose nanocrystal based electrospun nanofiber for biomedical applications-A review. Carbohydr Polym. 2025;348:122838. https://doi.org/10.1016/j.carbpol.2024.122838
28. Raghuwanshi VS, Garnier G. Nanoparticle decorated cellulose nanocrystals (CNC) composites for energy, catalysis, and biomedical applications. Adv Funct Mater. 2025;35(2):2412869. https://doi.org/10.1002/adfm.202412869
29. Antony Jose S, et al. A comprehensive review on cellulose Nanofibers, nanomaterials, and composites: Manufacturing, properties, and applications. Nanomaterials (Basel). 2025;15(5):356. https://doi.org/10.3390/nano15050356
30. Thach UD, Luu KN, Chung KL. Surface Modification of Nanocrystalline Cellulose for Optimized α-Mangostin Loading and Therapeutic Applications. ChemistrySelect. 2025;10(36):e01372. https://doi.org/10.1002/slct.202501372
31. Bhatnagar P, et al. Nanocrystalline Cellulose in Tissue Regeneration: Innovations, Challenges, and Future Directions. Regen Eng Transl Med. 2025:1-20.
32. Soltani M, et al. Targeted cancer therapy potential of quercetin-conjugated with folic acid-modified nanocrystalline cellulose nanoparticles: a study on AGS and A2780 cell lines. BMC Biotechnol. 2025;25(1):29. https://doi.org/10.1186/s12896-025-00962-w
33. Modarres M, Taghavizadeh Yazdi ME. Elicitation improves phenolic acid content and antioxidant enzymes activity in salvia leriifolia cell cultures. Iran J Sci Technol Trans Sci. 2021;45(3):849-855. https://doi.org/10.1007/s40995-021-01070-y
34. Nadaf M, Halimi Khalil Abad M, Gholami A, Taghavizadeh Yazdi ME, Iriti M, Mottaghipisheh J. Phenolic content and antioxidant activity of different Iranian populations of Anabasis aphylla L. Nat Prod Res. 2024 May;38(9):1606-1610. https://doi.org/10.1080/14786419.2022.2150621
35. Singh S, et al. Silibinin: a natural flavonoid with multifaceted anticancer potential and therapeutic challenges. Med Chem Res. 2025;34(7):1-22. https://doi.org/10.1007/s00044-025-03466-6
36. Sharma A, et al. Anticancer therapeutic potential of silibinin: current trends, scope and relevance. Med Chem Res. 2025;34(5):1-16. https://doi.org/10.1007/s00044-025-03383-8
37. He S, et al. Therapeutic potential and mechanistic insights of silibinin targeting cancer-associated fibroblasts in colorectal cancer. Front Pharmacol. 2025;16:1527871. https://doi.org/10.3389/fphar.2025.1527871
38. Borji S, et al. Enhanced therapeutic efficacy of silibinin loaded silica coated magnetic nanocomposites against Pseudomonas aeruginosa in Combination with Ciprofloxacin and HepG2 cancer cells. Sci Rep. 2025;15(1):21498. https://doi.org/10.1038/s41598-025-07529-x
39. Yazdi MET, et al. Biosynthesis, characterization, and antibacterial activity of silver nanoparticles using Rheum turkestanicum shoots extract. Res Chem Intermed. 2018;44(2):1325-1334. https://doi.org/10.1007/s11164-017-3169-z
40. Mobaraki F, et al. Apoptotic, antioxidant and cytotoxic properties of synthesized AgNPs using green tea against human testicular embryonic cancer stem cells. Process Biochem. 2022;119:106-118. https://doi.org/10.1016/j.procbio.2022.05.021
41. Ashna M, et al. Greener synthesis of cerium oxide nanoemulsion using pollen grains of Brassica napus and evaluation of its antitumour and cytotoxicity properties. Mater Technol. 2022;37(8):525-532. https://doi.org/10.1080/10667857.2020.1863558
42. Shamasi Z, et al. Role of Rubia tinctorum in the synthesis of zinc oxide nanoparticles and apoptosis induction in breast cancer cell line. Nanomed J. 2021;8(1):65-72. https://doi.org/10.22038/nmj.2021.08.07
43. Ray PP, et al. A comprehensive evaluation of the therapeutic potential of silibinin: a ray of hope in cancer treatment. Front Pharmacol. 2024;15:1349745. https://doi.org/10.3389/fphar.2024.1349745
44. Kumari P, et al. Enzymatic synthesis of cellulose nanocrystals from lemongrass and its application in improving anti-cancer drug release, uptake and efficacy. Ind Crops Prod. 2023;192:115933. https://doi.org/10.1016/j.indcrop.2022.115933
45. Xing R, et al. Efficient in vitro delivery of paclitaxel by a nanocellulose-coated dendritic mesoporous organosilica nanoparticle for enhanced chemodynamic cancer therapy. J Drug Deliv Sci Technol. 2023;86:104654. https://doi.org/10.1016/j.jddst.2023.104654
46. Sajjadiyan SZ, et al. Preparation of silibinin loaded pegylated niosomal nanoparticles and investigation of its effect on MCF-10A human breast cancer cell line. Der Pharmacia Lettre. 2016;8(16):70-75.
47. Pirouzpanah M, et al. The effects of silibinin on the induction of apoptosis and inhibition of cell growth in MCF-7 breast cancer cell line. Iran J Nutr Sci Food Technol. 2015;9(4):1-10.
48. Mahmoodi N, Motamed N, Paylakhi SH. The comparison of the effects of silybin and silybin-phosphatidylcholine on viability and ESR expression in human breast cancer T47D cell line. Cell J. 2014;16(3):299-308.
49. Jackson JK, et al. The use of nanocrystalline cellulose for the binding and controlled release of drugs. Int J Nanomedicine. 2011;6:321-330. https://doi.org/10.2147/IJN.S16749